Solvent-Controlled Metal Ion Binding Selectivity and Anion Interaction of the Acridinedione-Based Heteroditopic Host

P. Ashokkumar, V. T. Ramakrishnan, and P. Ramamurthy*

National Centre for Ultrafast Processes, University of Madras, Taramani Campus, Chennai- 600 113, India

Received: August 15, 2010; Revised Manuscript Received: November 21, 2010

Acridinedione-based heteroditopic hosts **1a**−**c**, which contain a flexible oxyethylene moiety as a metal ion binding site and amino hydrogen as an anion receptor unit, were synthesized and characterized. Metal ion and anion binding studies were carried out in different solvents to understand the solvent-induced selectivity of the metal ion binding and anion interactions. In acetonitrile, Ca^{2+} alone shows a binding with the oxyethylene unit and $-OCH_3$ group, which results in a fluorescence enhancement without any spectral shift due to the suppression of the photoinduced electron transfer (PET) process. In chloroform, in addition to Ca^{2+}, Na^+ also shows a fluorescence enhancement with a 14 nm red shift in the emission maximum. ^{1}H NMR titration studies confirm that the addition of Na^+ does not involve binding at the oxyethylene moiety, while it shows a binding at the acridinedione carbonyl group and $-OCH_3$ group, which results in the red shift and fluorescence enhancement, respectively. In the anion interaction studies, F^- shows a neat deprotonation in polar aprotic solvents, whereas in chloroform, it shows a H-bond complex due to the lower anion desolvation energy. The present study clearly signifies the role of solvent in metal ion selectivity, which is an often unnoticed parameter in metal ion binding.

I. Introduction

Molecular recognition is the first step in the design of molecular sensors for detection of ions or neutral species in organic or aqueous media.[1] In the presence of target species, the molecular sensor is designed to exhibit a physical response which must be easily measured. Among various detection techniques, fluorescence makes the best choice since it offers high sensitivity, fast response, easy online detection, and local observation by fluorescence imaging with subnanometer spatial resolution.[2] Furthermore, remote sensing is also possible by means of optical fibers with a molecular sensor immobilized at the tip.[3] High selectivity is a hallmark of biological receptors and has always been a most important aim of synthetic supramolecular chemistry.[4] Since Pedersen's initial observations,[5] on the affinity of macrocyclic polyethers to alkali and alkaline earth metal ions, several new types of ligands of similar structure have been synthesized to increase the stability of the cation−crown complex or to improve the cation selectivity of the ligand. Even though a large number of cyclic crown-ethers and related macrocyclic-based chemosensors were reported, the corresponding acyclic polyether-based sensors are relatively rare.[6−11] Among the early reports on acyclic polyether-based receptors, reported by Nakamura et al. and Ajayaghosh et al., the signaling of the binding event was achieved by excimer formation,[7] exciton interaction,[8] the twisted intramolecular charge transfer (TICT)[9] process, and the electron[10] or energy transfer[11] process between two terminal chromophore units. Recently, we have reported a photoinduced electron transfer (PET) based acyclic polyether linked acridinedione (ADD) derivative as a specific Ca^{2+} sensor.[12]

Cyclic crown ethers display a wide range of binding specificities, and the association properties of crown ethers with alkali and alkaline earth metal ions have been mainly described in terms of similarities between metal ion size and the size of the inner hole of the crown ether and also charge density of the metal ion.[13] Whereas, in pseudocyclic systems, combined effects of the size of the pseudocrown ether cavity, number of oxygen atoms, the charge density, and the coordination number of the cations play a considerable role in the selectivity of metal ion binding.[8b] Unlike cyclic crown ethers which are rigid, the acyclic polyether changes its conformation from linear to pseudocyclic structure upon variation in the solvent polarity or complex formation with metal ions.[7−9] Solvent-dependent conformational changes in poly(oxoethylene) linkers were investigated by theoretical as well as experimental methods.[14] It is reported that the carbon−carbon bond of the $-OCH_2CH_2O-$ unit exists predominantly in the gauche conformation in a high polar medium but shifts to the trans conformation in a low polar medium.[15] Accordingly, it has been suggested that the poly(oxoethylene) chain forms a pseudo lipophilic hydrocarbon core in low polar media, and in contrast, a pseudo hydrophilic electron-rich cavity is formed in highly polar media. However, until now, the effect of solvent on metal ion binding selectivity of the acyclic polyether receptors has scarcely been investigated. Herein, we report the solvent-controlled metal ion selectivity of an ADD-linked ditopic receptor, which contains acyclic polyether as a metal ion binding site and amino hydrogen as an anion receptor.

Anion recognition by neutral receptors through H-bonding interactions stays at the basis of many important subdisciplines of supramolecular chemistry.[16] Both H-bonding and deprotonation processes are involved in anion interaction, which depends on the basicity of the anion and acidity of the proton,[17] which in turn is determined by the solvent employed in the investigation. If the solvent polarity is high enough, it will lead to deprotonation by highly basic anions due to the higher anion desolvation energy.[17d] To better understand the role of solvent on the anion recognition ability of amino hydrogen, we have carried out anion binding studies of a heteroditopic host in

* Corresponding author. Fax: 091-44-24546709. Tel.: 091-44-24540962. E-mail: prm60@hotmail.com.

10.1021/jp107717z
Published on Web 12/15/2010

SCHEME 1: Synthetic Routes to Compounds 1a−c

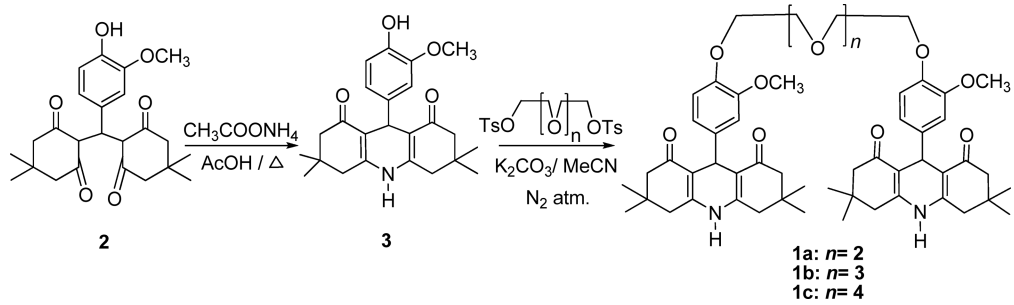

different solvents. Simultaneous binding of both metal ions and anions can be achieved with the use of a heteroditopic host, which contains two different receptors for two kinds of ions.[18] Since the present system consists of two distinct binding sites for metal ions and anions, we have also carried out the effect of competing anion on the binding ability of metal ions and vice versa.

II. Experimental Methods

All starting materials and reagents were purchased from commercial suppliers and used without further purification. The solvents used for the spectral studies were of HPLC grade. Absorption spectra were recorded on an Agilent 8453 diode array spectrophotometer. Emission spectra were recorded on a HORIBA JOBIN YVON Fluoromax 4P spectrophotometer. The fluorescence quantum yield was determined by exciting the sample at 366 nm with the use of quinine sulfate as the standard ($\phi_f = 0.546$ in 0.1 N H_2SO_4). Fluorescence decays were recorded by using an IBH time-correlated single-photon counting technique as reported elsewhere.[19] NMR spectra were recorded on JEOL 500 MHz and Bruker Avance III 500 MHz instruments in deuterated solvents as indicated. Chemical shifts are reported in parts per million, and coupling constants ($J_{X-X'}$) are reported in hertz. ESI−MS were performed on an ECA LCQ Thermo system with ion-trap detection in positive and negative mode. Elemental analyses (C, H, and N) were taken on a Euro EA Elemental analyzer.

General Procedure for Ion Binding Studies. Bichromophores **1a−c** were dissolved in the respective solvents. Metal perchlorate stock solutions (9.11×10^{-3} M) were prepared in acetonitrile (due to the solubility reason), and the titrations were carried out by adding small volumes (1−5 μL) of the metal ion to the bichromophore (3.5 mL) in a quartz cuvette. After the addition of metal ion to the cuvette, using a microliter syringe, the solution was shaken well and kept for 1 min before recording any measurements. To clarify the effect of added acetonitrile to the chloroform solution of bichromophore **1a−c**, we have also purposely carried out a blank experiment by adding 1−5 μL of acetonitrile to the chloroform solution of dyes. The addition of acetonitrile did not show any change in all the experiments, which shows the absence of any influence by the added solvent. For ^{1}H NMR titration studies, 1−7 μL of metal ions in CD_3CN was added to a 4.0 mM solution of bichromophores in $CDCl_3$. Anions were used as their tetrabutylammonium salts. Stock solutions of anions (0.07 M for experiments in low polar solvents and 0.24 M for polar solvents) were prepared in acetonitrile. Complex stoichiometry has been determined from the continuous variation technique (Job plot),[20] based on the difference in fluorescence intensity ΔF ($\Delta F = F_0 - F$) of bichromophores observed in the presence of metal ions or anions. Equimolar solutions of **1a** and metal ions were prepared and mixed to standard volumes and proportions so that the total concentration remained constant. ΔF values were calculated by measuring the fluorescence intensity of bichromophores in the absence (F_0) and presence (F) of the corresponding concentration of metal ions or anions. Subsequently, ΔF values were plotted for the corresponding metal ion against mole fraction (x_i = [bichromophore]/([bichromophore] + [metal ion])).

General Procedure of Synthesis of 1a−c. The synthesis of ditopic hosts **1a−c** is outlined in Scheme 1.[12a] The acridinedione **3** was obtained by refluxing tetraketone with ammonium acetate in acetic acid. Reaction of acridinedione with the corresponding ditosylate in the presence of K_2CO_3 yielded bisacridinediones **1a−c**, which were characterized by spectral analyses.

***9,9′-(4,4′(2,2′(Ethylenedioxy-bis(ethyleneoxy)))-bis(3-methoxyphenyl))bis(3,3,6,6-tetramethyl-3,4,6,7,9,10-hexahydro-1,8(2H,5H) Acridinedione)* (1a).** Yield, 62%; mp, 143−145 °C; FTIR (KBr) (cm^{-1}) 3194 (NH), 1639 (CO), 1485 (−C═C−); ^{1}H NMR (500 MHz; $CDCl_3$:DMSO-d_6, TMS) δ (ppm) = 8.77 (2H, s, NH), 6.90 (2H, d, J = 1.8 Hz, ArH), 6.70−6.73 (4H, m, ArH), 4.93 (2H, s, C_9−H), 4.04 (4H, t, OCH_2), 3.76−3.78 (10H, m, OCH_2 and OCH_3), 3.66 (4H, s, OCH_2), 2.39 and 2.10 (8H, 2 d, J = 16.8 Hz, C_2 & C_7 −CH_2), 2.24 and 2.15 (8H, 2 d, J = 16.0 Hz, C_4 & C_5 −CH_2), 1.07 and 0.95 (24H, 2s, *gem*-dimethyl); ^{13}C NMR (125 MHz; $CDCl_3$, DMSO-d_6, TMS) δ (ppm) = 195.6 (CO), 149.1 (C═C), 148.7 (C), 145.9 (C), 140.6 (C), 119.7 (CH), 113.3 (CH), 112.5 (CH), 112.4 (C═C), 70.4 (CH_2), 69.4 (CH_2), 68.3 (CH_2), 55.6 (CH_3), 50.7 (CH_2), 40.1 (CH_2), 32.6 (C), 32.3 (CH), 29.5 and 26.8 (CH_3); MS (ESI) m/z = 906.19 [M + 1]$^+$. Elemental analysis (%) calcd for $C_{54}H_{68}N_2O_{10}$ (905.12): C, 71.66; H, 7.57; N, 3.09. Found: C, 71.72; H, 7.54; N, 3.06.

***9,9′-(4,4′(2,2′(Oxybis(3-oxapentamethleneoxy)))-bis(3-methoxyphenyl))bis(3,3,6,6-tetramethyl-3,4,6,7,9,10-hexahydro-1,8(2H,5H) Acridinedione)* (1b).** Yield, 58%; mp 129−131 °C; FTIR (KBr) (cm^{-1}) 3194 (NH), 1640 (CO), 1486 (−C═C−); ^{1}H NMR (500 MHz; $CDCl_3$, TMS) δ (ppm) = 8.74 (2H, s, NH), 6.91 (2H, d, J = 1.8 Hz, ArH), 6.64−6.70 (4H, m, ArH), 4.98 (2H, s, C_9−H), 4.02 (4H, t, OCH_2), 3.70−3.76 (10H, m, OCH_2 and OCH_3), 3.59−3.64 (4H, m, OCH2), 3.57 (4H, s, OCH_2), 2.30 and 2.16 (8H, 2 d, J = 16.0 Hz, C_2 & C_7 −CH_2), 2.27 and 2.11 (8H, 2 d, J = 16.5 Hz, C_4 & C_5 −CH_2), 1.01 and 0.91 (24H, 2s, *gem*-dimethyl); ^{13}C NMR (500 MHz; $CDCl_3$, TMS) δ (ppm) = 195.9 (CO), 149.4 (C═C), 148.7 (C), 146.3 (C), 140.7 (C), 119.8 (CH), 113.2 (CH), 113.0 (CH), 112.4 (C═C), 70.6 (CH_2), 70.2 (CH_2), 68.3 (CH_2), 55.8 (CH_3), 50.8 (CH_2), 40.6 (CH_2), 32.5 (C), 32.4 (CH), 29.5 and 27.0 (CH_3); MS (ESI) m/z = 950.23 [M + 1]$^+$. Elemental analysis (%) calcd for $C_{56}H_{72}N_2O_{11}$ (949.18): C, 70.86; H, 7.65; N, 2.95. Found: C, 70.94; H, 7.67; N, 2.92.

***9,9′-(4,4′(2,2′(Ethylenedioxybis(3-oxapentamethyleneoxy)))-bis(3-methoxyphenyl))bis(3,3,6,6-tetramethyl-3,4,6,7,9,10-hexahydro-1,8(2H,5H) Acridinedione)* (1c).** Yield, 57%; mp 117−119 °C; FTIR (KBr) (cm^{-1}) 3193 (NH), 1640 (CO), 1486 (−C═C−); ^{1}H NMR (500 MHz; $CDCl_3$, TMS) δ (ppm) = 8.77 (2H, s, NH), 6.98 (2H, d, J = 1.8 Hz, ArH), 6.72−6.78 (4H, m, ArH), 5.04 (2H, s, C_9−H), 4.04 (4H, t, OCH_2), 3.78−3.81 (10H, m, OCH_2 and OCH_3), 3.64−3.67 (8H, m, OCH_2), 3.63 (4H, s, OCH_2), 2.34 and 2.21 (8H, 2 d, J = 16.5 and 16.0 Hz C_2 & C_7 $-CH_2$), 2.23 and 2.16 (8H, 2 d, J = 16.5 Hz, C_4 & C_5 $-CH_2$), 1.06 and 0.96 (24H, 2s, *gem*-dimethyl); ^{13}C NMR (500 MHz; $CDCl_3$, TMS) δ (ppm) = 195.6 (CO), 149.0 (C═C), 148.7 (C), 145.9 (C), 140.6 (C), 119.7 (CH), 113.2 (CH), 112.6 (CH), 112.4 (C═C), 70.4 (CH_2), 70.2 (CH_2), 69.3 (CH_2), 68.3 (CH_2), 55.6 (CH_3), 50.8 (CH_2), 40.5 (CH_2), 32.6 (C), 32.3 (CH), 29.5 and 26.9 (CH_3); MS (ESI) m/z = 994.27 $[M + 1]^+$. Elemental analysis (%) calcd for $C_{58}H_{76}N_2O_{12}$ (993.23): C, 70.14; H, 7.71; N, 2.82. Found: C, 70.17; H, 7.68; N, 2.80.

III. Results and Discussion

a. Photophysical Studies. Compounds **1a**−**c** show the absorption and emission maxima around 361 and 426 nm, respectively, which are assigned to the intramolecular charge transfer (ICT) from the ring nitrogen atom to the ring carbonyl center within the ADD moiety. Lower fluorescence quantum yield (ϕ_f = 0.039 ± 5%) and lifetime (biexponential: 0.26 ± 0.01 ns (22.3%) and 2.40 ± 0.03 ns (77.7%)) of **1a**−**c** in acetonitrile, compared to the constituent fluorophore without the electron donor $-OCH_3$ group (ϕ_f = 0.21 ± 2% and τ_f = 2.01 ± 0.03 ns in acetonitrile), are attributed to the intramolecular PET process through space from the electron-rich $-OCH_3$ group to the relatively electron-deficient excited state of the ADD fluorophore.[12,19] The bichromophores show relatively lower quantum yield (ϕ_f = 0.018 ± 5%) and lifetime (biexponential: 0.14 ± 0.01 ns (68.5%) and 2.29 ± 0.03 ns (31.5%)) in chloroform compared to acetonitrile due to the change in the polarity of the medium. The earlier reported[12a] bichromophores having a $-CH_3$ group instead of H at the ring nitrogen (ICT donor) showed relatively higher quantum yield and lifetime due to the enhanced ICT from the electron-releasing $-CH_3$ group.

b. Metal Ion Binding Studies. Among the metal ions investigated in acetonitrile, the oxyethylene receptor shows selective binding with Ca^{2+}. Addition of Ca^{2+} results in the 3 nm red-shifted absorption maximum (Figure S1, Supporting Information) and 6-fold fluorescence enhancement without any spectral shift as shown in Figure 1. Addition of other metal ions like Na^+, K^+, and Mg^{2+} did not show any considerable change in both absorption and emission spectra, which is evident from the metal ion selectivity plot (Figure 2). Binding of Ca^{2+} at the oxyethylene moiety and $-OCH_3$ group suppresses the PET process and results in the fluorescence enhancement without any spectral shift as observed earlier for the similar compound.[12]

In chloroform, both Na^+ and Ca^{2+} show spectral changes, which were analyzed thoroughly. Addition of Ca^{2+} to **1a** in chloroform did not show any considerable shift in the absorption maximum (Figure S2, Supporting Information). The corresponding fluorescence spectrum shows 8.5-fold enhancement in the intensity without any spectral shift as shown in Figure 3. The absence of any spectral shift indicates that the Ca^{2+} did not involve any interaction with the carbonyl group of the ADD moiety, which is an acceptor in the ICT electronic transition. On the other hand, the addition of Na^+ to chloroform solution

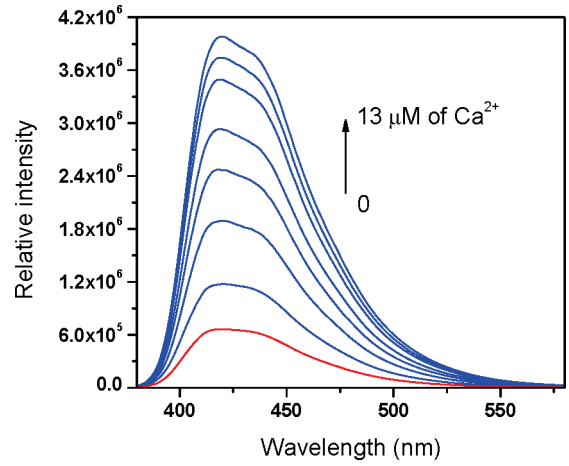

Figure 1. Fluorescence spectra of **1a** (11 μM) upon addition of Ca^{2+} in acetonitrile; λ_{ex} = 363 nm.

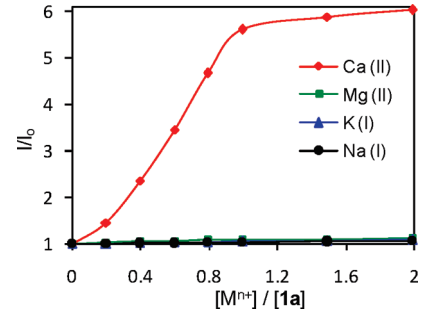

Figure 2. Metal ion selectivity plot of **1a** (11 μM) upon addition of different metal ions in acetonitrile; λ_{ex} = 363 nm.

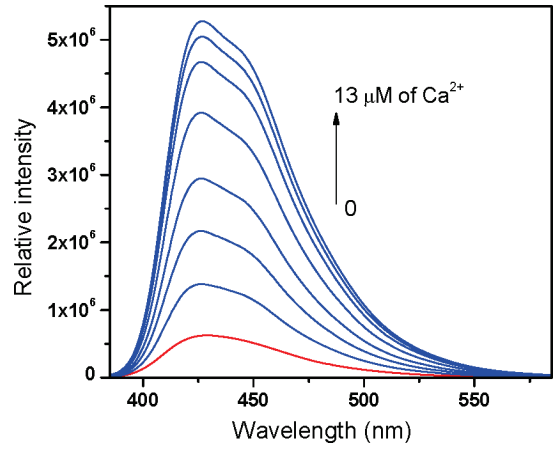

Figure 3. Fluorescence spectra of **1a** (11 μM) upon addition of Ca^{2+} in chloroform; λ_{ex} = 363 nm.

of **1a** shows a 9 nm red-shifted absorption maximum with an isosbestic point at 371 nm as shown in Figure 4a. The existence of a clear isosbestic point indicates the presence of 1:1 complexation with Na^+. The corresponding emission spectrum (Figure 4b), when excited at its isosbestic point, shows a 14 nm red-shifted emission maximum together with an enhancement in the fluorescence intensity. Observation of a red shift in both absorption and emission spectra indicates the involvement of the ADD carbonyl group in Na^+ binding. To determine the stoichiometry of the complexes, a Job's plot[20] has been carried out from the changes in the fluorescence intensity. For both the metal ions, the Job's plot (Figure S3, Supporting Information) showed the maximum changes, when the mole fraction of **1a** was around 0.5, which is a characteristic of a host−guest binding

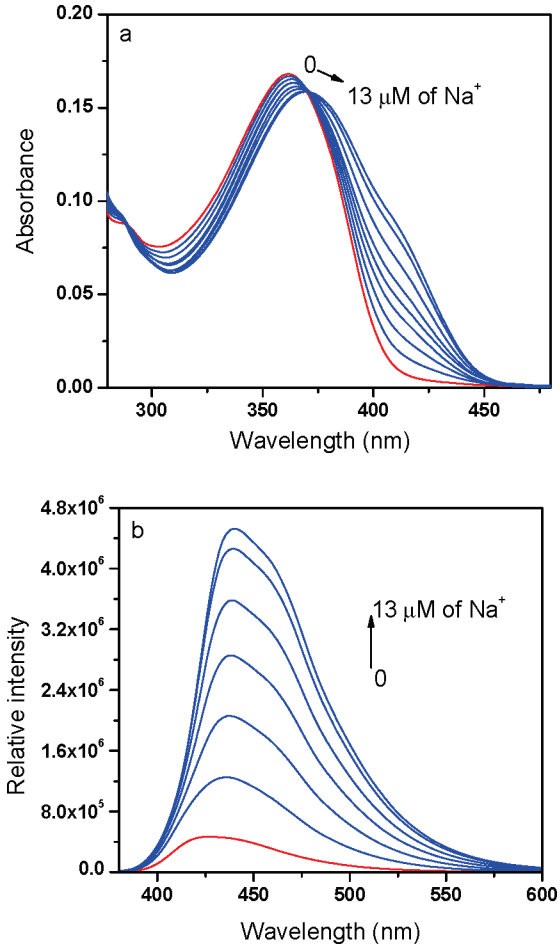

Figure 4. (a) Absorption and (b) fluorescence spectra of **1a** (11 μM) upon addition of Na^+ in chloroform; λ_{ex} = 371 nm.

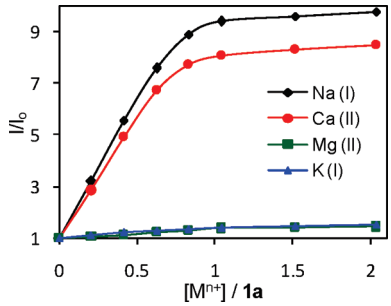

Figure 5. Metal ion selectivity plot of **1a** (11 μM) upon addition of different metal ions in chloroform; λ_{ex} = 371 nm.

in a 1:1 stoichiometry. Quantitative binding constant values could not be obtained accurately due to the possibility of the ion-pair formation in less polar organic solvents. Addition of K^+ and Mg^{2+} did not show any considerable change in both absorption and emission spectra, which is clear from the plot (Figure 5) of fluorescence intensity against the ratio of the metal ion and **1a**. Metal ion binding studies of other derivatives **1b** and **1c** also showed behavior similar to that observed in **1a**. Similar metal ion binding behavior is observed in other less polar solvents, namely, toluene (Figure S4, Supporting Information) and dichloromethane (Figure S5, Supporting Information), which suggest that the polarity of the solvent plays a major role in the metal ion interaction of acyclic polyether-based receptors.

The complex formation between metal ions and **1a** has also been investigated by time-resolved fluorescence studies. Bichromophore **1a**

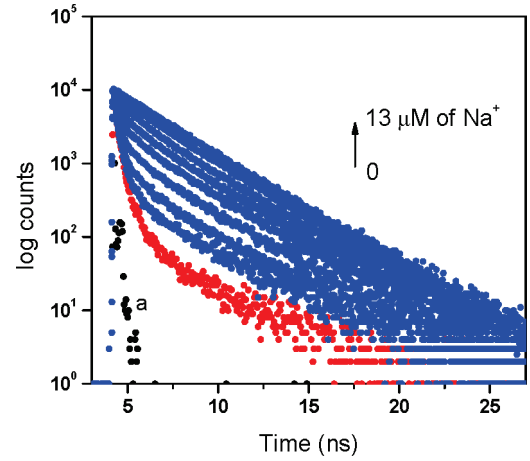

Figure 6. Fluorescence decay profiles of **1a** (11 μM) upon addition of Na^+ in chloroform; λ_{ex} = 371 nm and λ_{em} = 440 nm. (a) Laser profile.

shows a biexponential decay with a PET quenched lifetime of 0.14 ns (68.1%) and 2.25 ns (31.9%) in chloroform. Addition of Na^+ (Figure 6) to the chloroform solution of **1a** shows a gradual disappearance of a shorter-lifetime component with the increase in the lifetime (2.25 to 3.09 ns) and amplitude of the longer component. The disappearance of the shorter lifetime component confirms the suppression of the PET process in the Na^+-bound complex of **1a**. We observe a single exponential decay with longer lifetime (3.09 ns) on complete complex formation with Na^+. Addition of Ca^{2+} (Figure S6, Supporting Information) also shows a similar behavior with the longer lifetime being 2.86 ns.

To unravel the binding mode of metal ions, ^{1}H NMR titration studies were carried out in $CDCl_3$. Addition of Na^+ (Figure 7) to the bichromophore **1a** did not show any significant change in the oxyethylene proton peaks, which shows the absence of binding at the oxyethylene moiety. In contrast, the $-OCH_3$ proton peak *i* shifted ($\Delta\delta$ = 0.60) to higher magnetic field due to the decreased deshielding effect of the metal-coordinated oxygen atom of the $-OCH_3$ group. The aromatic proton peak *g* shifted ($\Delta\delta$ = 0.16) toward a lower magnetic field due to the decreased electron density at the oxygen atom of the OCH_3 group. Aromatic proton *h* nearest to the Na^+ binding site shifted ($\Delta\delta$ = 0.26) to higher magnetic field due to the shielding effect of the counteranion, perchlorate. The acridinedione proton peaks *k* and *l* nearest to the ADD carbonyl group shifted ($\Delta\delta$ = 0.14 and 0.35) to lower magnetic field due to the deshielding effect of the electron-deficient carbonyl carbon. Binding of Na^+ at the carbonyl oxygen decreases the electron density on the carbonyl group, which creates electron deficiency at the carbonyl carbon. The above changes clearly confirm that the Na^+ involves binding at the $-OCH_3$ and ADD carbonyl group as shown in Scheme 2.

Binding of Na^+ at the carbonyl group increases the ICT character of the electronic transition, which results in the red shift in both absorption and emission maxima. In addition, binding at the $-OCH_3$ group suppresses the PET process and results in the fluorescence enhancement.

Addition of Ca^{2+} (Figure 8) to bichromophore **1a**[21] shows a lower magnetic field shift of the oxyethylene proton peaks *c* ($\Delta\delta$ = 0.10) and *d* ($\Delta\delta$ = 0.03) which indicates the binding of Ca^{2+} at the middle oxygen atoms of the oxyethylene receptor. The observed higher magnetic field shift of $-OCH_3$ proton peak *i* ($\Delta\delta$ = 0.09) indicates the binding at the OCH_3 group. Aromatic protons show a similar shift as observed in the case of Na^+;

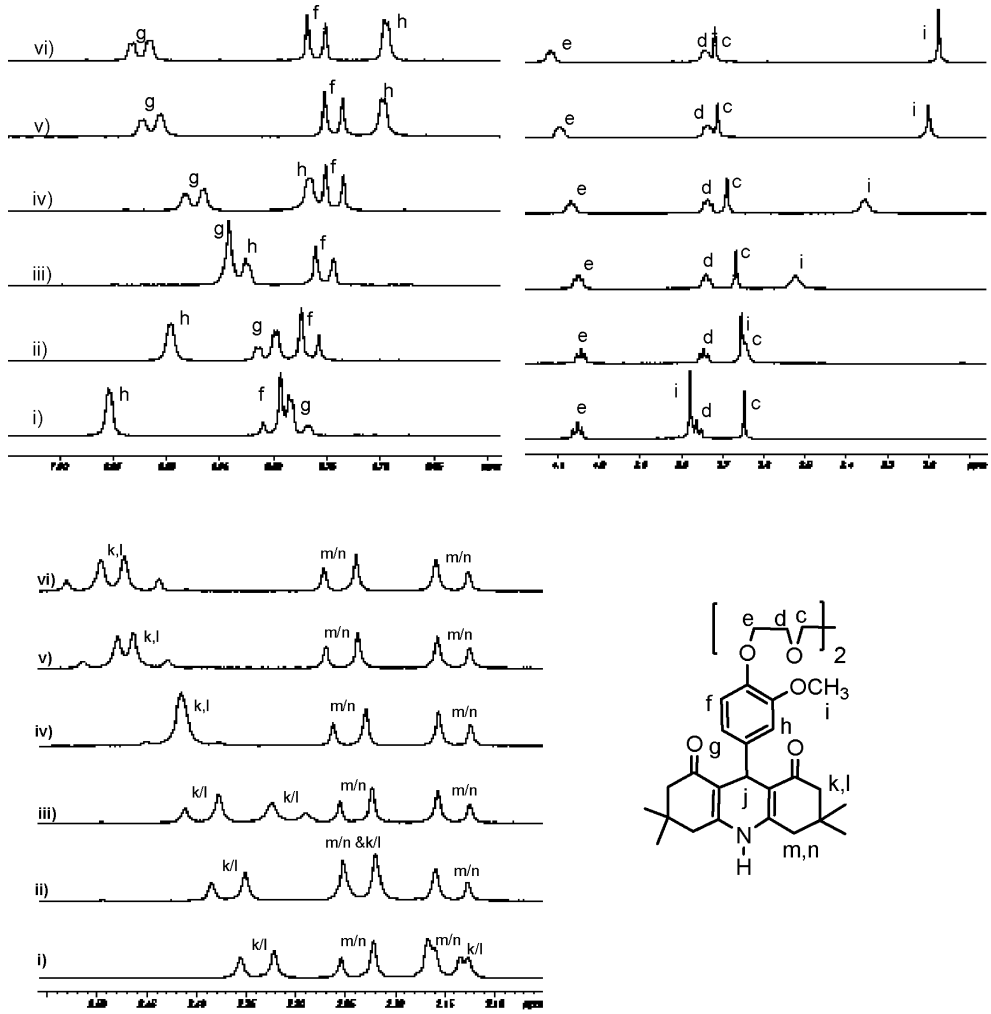

Figure 7. Partial ^{1}H NMR spectra of **1a** in $CDCl_3$ upon addition of (i) 0, (ii) 0.2, (iii) 0.4, (iv) 0.6, (v) 0.8, and (vi) 1.0 equiv of Na^+.

SCHEME 2: Binding Mode of Na^+ with 1a in Chloroform

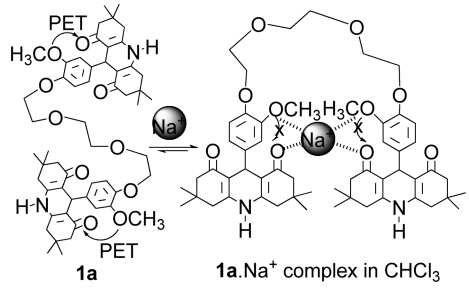

however, the peaks are considerably broadened due to the turbidity of the solution, and the extent of shift was found to be relatively low. The absence of any shift of acridinedione proton peaks *k* and *l* in the ^{1}H NMR indicates the absence of Ca^{2+} binding at the ADD carbonyl group. The absence of a red shift in both absorption and emission spectral studies is in line with the observed NMR spectral changes, which reveals that the Ca^{2+} binds at the middle oxygen atoms of the oxyethylene moiety and the $-OCH_3$ group as shown in Scheme 3. Binding of Ca^{2+} at the oxyethylene moiety and the $-OCH_3$ group results in the suppression of the PET process and fluorescence enhancement without any spectral shift.[12]

c. Anion Binding Studies. Addition of AcO^- to a chloroform solution of **1a** shows an 8 nm red-shifted absorption maximum (Figure S7, Supporting Information), which indicates the H-bonding interaction of AcO^- with an amino hydrogen. The corresponding fluorescence spectrum shows a 17 nm red-shifted emission peak with fluorescence enhancement as shown in Figure 9. Addition of $H_2PO_4^-$ also shows a similar behavior with a 6 nm red-shifted absorption maximum and a 12 nm red-shifted emission maximum with fluorescence enhancement (Figure S8, Supporting Information). A similar change has been observed in polar aprotic solvents like acetronitrile, dimethyl formamide, and dimethyl sulfoxide for AcO^- and $H_2PO_4^-$, but the extent of red shift was found to be higher due to the increased polarity of the medium.[22]

Addition of F^- to an acetonitrile solution of **1a** shows a decrease in the absorbance at 365 nm with the simultaneous appearance of a new peak at 457 nm (Figure 10a). The corresponding emission spectrum shows a decrease in the emission intensity at a 427 nm peak with formation of a new emission peak at 505 nm (Figure 10b). As the smallest and highly electronegative anion, F^- deprotonates the amino hydrogen, which results in the formation of a new peak in both absorption and emission spectra in polar aprotic solvents.[22] In contrast, the addition of F^- to **1a** in low polar aprotic solvents like chloroform, dichloromethane, and toluene did not show any new peak in both absorption and emission spectra. Addition of F^- to a chloroform solution of **1a** shows a 17 nm red-shifted absorption maximum as shown in Figure 11a. The corresponding emission spectra show a 32 nm red-shifted emission maximum together with fluorescence enhancement (Figure 11b). Binding

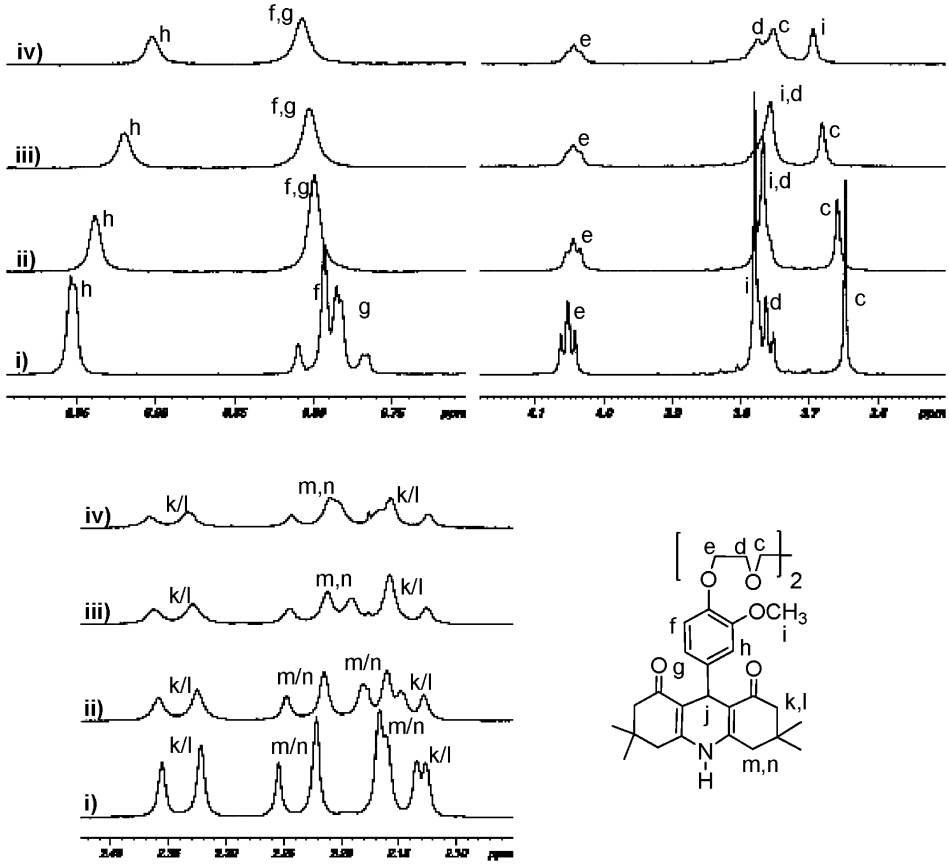

Figure 8. Partial ^{1}H NMR spectra of **1a** in $CDCl_3$ upon addition of (i) 0, (ii) 0.2, (iii) 0.5, and (iv) 1.0 equiv of Ca^{2+}.

SCHEME 3: Binding Mode of Ca^{2+} with 1a in Chloroform

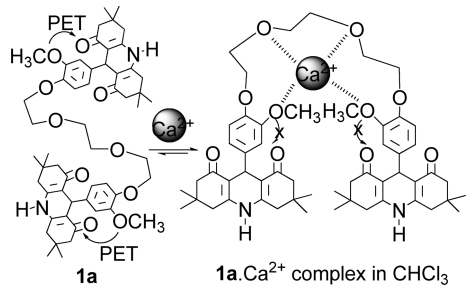

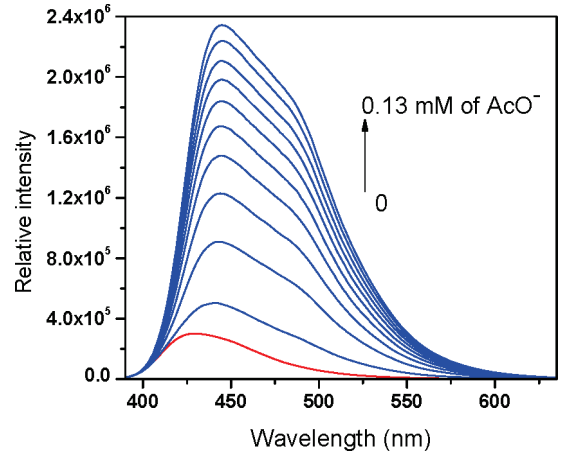

Figure 9. Fluorescence spectra of **1a** (12 μM) upon addition of AcO^- in chloroform; λ_{ex} = 362 nm.

ratio of 1:2 (dye:anion) were proved from a Job's plot (Figure S9, Supporting Information) analysis, which showed maximum fluorescence intensity changes when the mole fraction of **1a** was around 0.33. The fluorescence spectral changes of **1a** with the addition of F^- in toluene and DCM are presented in Figures S10 and S11 (Supporting Information), respectively. The observed difference in the spectral response of F^- in chloroform compared to acetonitrile may be due to the absence of deprotonation of an amino hydrogen in chloroform. To confirm this, we have carried out similar experiments in chloroform with the addition of OH^-, which is a well-known deprotonating agent. Addition of OH^- to a chloroform solution of **1a** shows a decrease in the absorbance at 361 nm with the formation of a new absorption peak at 453 nm (Figure S12a, Supporting Information). In emission spectral studies, also a new peak is formed at 500 nm (Figure S12b, Supporting Information). This clearly proves that the deprotonated form of dye absorbs and emits at 453 and 500 nm, respectively, in chloroform. So, the observed red shift in absorption and emission spectra of **1a** with F^- is due to the H-bonding complexation with the amino hydrogen. The decreased anion desolvation energy in chloroform leads to the formation of a stable H-bond complex instead of deprotonation by F^-. H-bonding interaction of anions with amino hydrogen increases the electron density of the ICT donor, which in turn leads to the red shift in both absorption and emission maxima together with an increase in the intensity. The extent of red shift depends on the charge density of anions, which accounts for the observed red shift for F^-, AcO^-, and $H_2PO_4^-$. So, by changing the polarity of the medium, one can tune the anion-receptor H-bonding complexation and deprotonation of the receptor. Addition of other anions like Cl^-, Br^-, I^-, HSO_4^-, and ClO_4^- did not show any such changes in both absorption and emission spectra.

The complexation between anions and **1a** has also been investigated by time-resolved fluorescence studies. Addition of

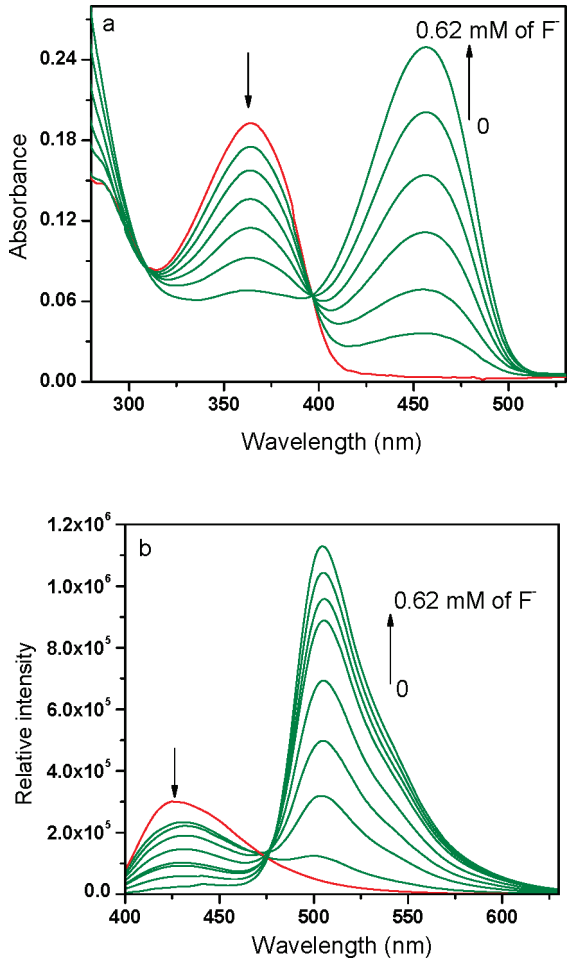

Figure 10. (a) Absorption and (b) fluorescence spectra of **1a** (12 μM) upon addition of F^- in acetonitrile; λ_{ex} = 395 nm.

F^- to a chloroform solution of **1a** shows a triexponential decay as shown in Figure 12. Both the lifetime components of free dye decrease with the formation of a longer-lifetime (6.59 ns) component. We observed a single exponential decay with longer lifetime component on complete complex formation with F^-. Addition of AcO^- and $H_2PO_4^-$ also shows a similar behavior, the longer lifetime being 4.69 and 4.18 ns, respectively. The observed enhancement in the lifetime also follows the order of the basicity of the anion.

d. Simultaneous Binding Studies of Metal Ions and Anions. To understand the binding ability of an ion in the presence of its competing ion, we have carried out two sets of simultaneous binding studies of **1a** with metal ions and anions. First, we have titrated **1a** with anion in the presence of metal ion. Figure 13 shows the absorption and emission spectra of the **1a**·Na^+ complex with the addition of F^-. As can be seen, the addition of 1 equiv of F^- brings back the red-shifted absorption maximum of **1a** to 361 nm. This suggests the sequestering of the metal ion from the binding site and the existence of free dye **1a**. However, when sequestering of the metal ion is complete, further addition of F^- binds at the amino group and results in a red shift of the absorption maximum as observed in the anion binding studies, which is further confirmed by emission spectral studies. Up to 1 equiv of F^-, the emission intensity at 440 nm decreases and reaches the intensity of the free **1a** together with a shift from 440 to 426 nm; after the complete sequestering of Na^+, further addition leads to a 32 nm red-shifted emission peak with the increase in the intensity. These results confirm the sequestering of Na^+ by

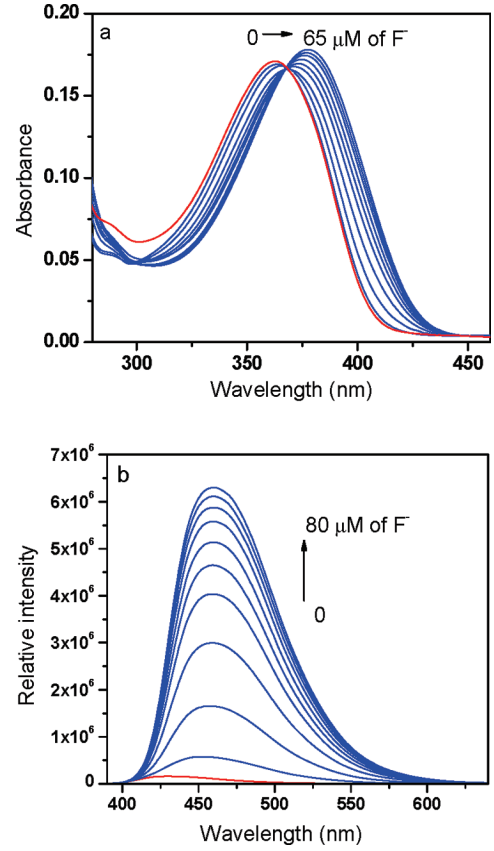

Figure 11. (a) Absorption and (b) fluorescence spectra of **1a** (11 μM) upon addition of F^- in chloroform; λ_{ex} = 368 nm.

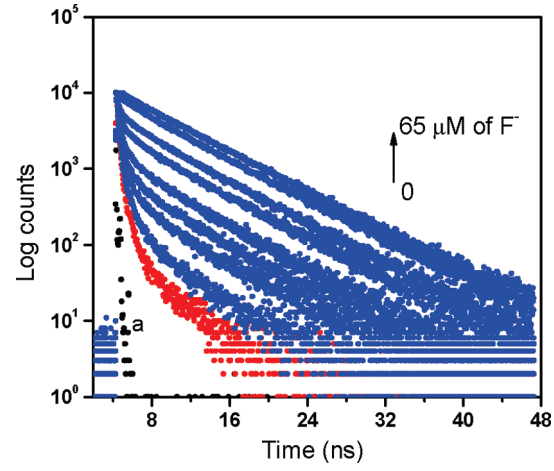

Figure 12. Fluorescence decay profiles of **1a** (11 μM) upon addition of F^- in chloroform; λ_{ex} = 370 nm and λ_{em} = 460 nm. (a) Laser profile.

the added F^- (Figure S13, Supporting Information). In the second experiment, Na^+ is titrated with the **1a**·F^- complex, which also shows a similar sequestering process (Figure S14, Supporting Information). Other metal Ca^{2+} ions and anions such as AcO^- and $H_2PO_4^-$ also show the sequestering process. Even though **1a** contains distinct binding sites for both metal ions and anions, positive cooperative binding of both types of analytes, as observed exploiting the allosteric effect,[23] through electrostatic interactions between the ion pairs[24] or to the host as an associated ion pair,[25] is not possible in this case due to the absence of close proximity of two binding sites.[26] The weak binding of the host−guest interaction and the strong ion-pairing equilibria between two types of ions lead to the sequestering of ions. In most organic solvents, the metal ions and anions do

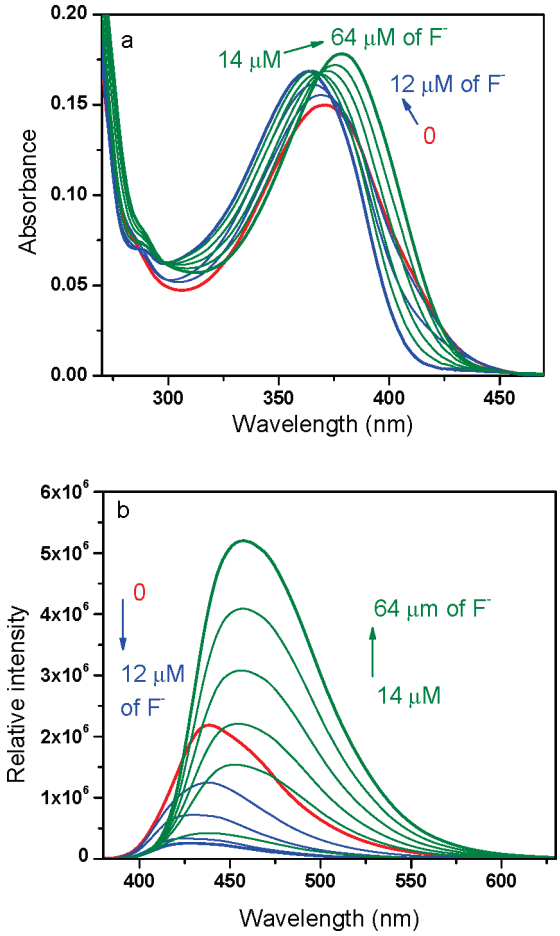

Figure 13. (a) Absorption and (b) fluorescence spectra of **1a** (11 μM) + Na^+ (11 μM) upon addition of F^- in chloroform; λ_{ex} = 371 nm.

not exist as free ions; instead, they are present as solvent separated ion pairs, contact ion pairs, and/or aggregated contact ion pairs.[27] Ion pairing between two types of ions decreases the host−guest binding ability, when the two kinds of receptors present far apart.

IV. Conclusion

We have shown that the binding mode of the metal ion and the selectivity toward an acyclic polyether-based receptor strongly depend on the nature of the solvent. In acetonitrile, Ca^{2+} alone shows the binding at the oxyethylene receptor unit and $-OCH_3$ groups, whereas in low polar aprotic solvents like chloroform, both Ca^{2+} and Na^+ are involved in the binding and result in the distinct optical output. The binding mode of metal ions with the receptor is proved from the ^1H NMR titration spectra. Addition of Na^+ is involved in the binding at the ADD carbonyl group and $-OCH_3$ group, which results in the red shift of both absorption and emission spectra together with an increase in the emission intensity. In contrast, Ca^{2+} involves binding at the middle oxygen atoms of the oxyethylene receptor and $-OCH_3$ group and leads to the fluorescence enhancement without any spectral shift. In anion binding studies, the reversal of H-bonding complexation and deprotonation is observed depending on the solvent polarity. In polar aprotic solvents, F^- induced deprotonation of amino hydrogen, whereas in low polar aprotic solvents, it forms a stable H-bond complex with the amino hydrogen. Simultaneous binding studies of metal ions and anions show the sequestering process due to the absence of cooperative binding between two different types of ions. Our finding clearly illustrates that the effect of solvent on ion recognition should also have been included in the design of selective metal ion and/or anion receptors.

Acknowledgment. We thank the Department of Science and Technology (DST), Government of India, for financial support through SERC scheme project no. DST/SR/S1/PC-31/2005. Financial support by DST-IRHPA is also gratefully acknowledged.

Supporting Information Available: NMR spectra of **1a**; absorption and emission spectra of **1a** with various metal ions and anions; Job's plot for **1a** toward metal ions and anions. This material is available free of charge via the Internet at http://pubs.acs.org.

References and Notes

(1) Dodziuk, H. *Introduction to Supramolecular Chemistry*; Kluwer Academic Publishers: Dordrecht, The Netherlands, 2001.

(2) (a) de Silva, P.; Gunaratne, H. Q. N.; Gunnlaugsson, T.; Huxley, A. J. M.; McCoy, C. P.; Rademacher, J. T.; Rice, T. E. *Chem. Rev.* **1997**, *97*, 1515–1566. (b) Valeur, B.; Leray, I. *Coord. Chem. Rev.* **2000**, *205*, 3–40.

(3) Desvergne, J. P.; Czarnik, A. W., Eds. *Chemosensors for Ion and Molecule Recognition*; Kluwer Academic Publishers: Dordrecht, The Netherlands, 1997.

(4) (a) Schneider, H.-J.; Yatsimirsky, A. *Principles and Methods in Supramolecular Chemistry*; Wiley: Chichester, 2000. (b) Steed, J.-W.; Atwood, J. L. *Supramolecular Chemistry*; Wiley: New York, 2000.

(5) (a) Pedersen, C. J. *J. Am. Chem. Soc.* **1967**, *89*, 7017–7036. (b) Pedersen, C. J.; Frensdorff, H. K. *Angew. Chem., Int. Ed. Engl.* **1972**, *11*, 16–25.

(6) (a) Tummler, B.; Maass, G.; Weber, E.; Wehner, W.; Vogtle, F. *J. Am. Chem. Soc.* **1977**, *99*, 4683–4690. (b) Lohr, H.-G.; Vogtle, F. *Acc. Chem. Res.* **1985**, *18*, 65–72. (c) Valeur, B.; Pouget, J.; Bourson, J.; Kaschke, M.; Ernsting, N. P. *J. Phys. Chem.* **1992**, *96*, 6545–6549. (d) Tahara, R.; Morozumi, T.; Suzuki, Y.; Kakizawa, Y.; Akita, T.; Nakamura, H. *J. Inclusion Phenom. Macrocycl. Chem.* **1998**, *32*, 283–294. (f) Liu, Y.; Duan, Z.-Y.; Zhang, H.-Y.; Jiang, X.-L.; Han, J.-R. *J. Org. Chem.* **2005**, *70*, 1450–1455.

(7) Suzuki, Y.; Morozumi, T.; Nakamura, H.; Shimomura, M.; Hayashita, T.; Bartsch, R. *J. Phys. Chem. B* **1998**, *102*, 7910–7917.

(8) (a) Ajayaghosh, A.; Arunkumar, E.; Daub, J. *Angew. Chem., Int. Ed.* **2002**, *41*, 1766–1769. (b) Arunkumar, E.; Ajayaghosh, A.; Daub, J. *J. Am. Chem. Soc.* **2005**, *127*, 3156–3164. (c) Arunkumar, E.; Chitra, P.; Ajayaghosh, A. *J. Am. Chem. Soc.* **2004**, *126*, 6590–6598.

(9) (a) Morozumi, T.; Anada, T.; Nakamura, H. *J. Phys. Chem. B* **2001**, *105*, 2923–2931. (b) Kim, J.; Morozumi, T.; Nakamura, H. *Org. Lett.* **2007**, *9*, 4419–4422.

(10) Tahara, R.; Hasebe, K.; Nakamura, H. *Chem. Lett.* **1995**, *24*, 753–754.

(11) Suzuki, Y.; Morozumi, T.; Kakizawa, Y.; Bartsch, R. A.; Hayashita, T.; Nakamura, H. *Chem. Lett.* **1996**, *25*, 547–548.

(12) (a) Ashokkumar, P.; Ramakrishnan, V. T.; Ramamurthy, P. *Eur. J. Org. Chem.* **2009**, 5941–5947. (b) Velu, R.; Ashokkumar, P.; Ramakrishnan, V. T.; Ramamurthy, P. *Tetrahedron Lett.* **2010**, *51*, 3102–3105.

(13) (a) Michaux, G.; Reisse, J. *J. Am. Chem. Soc.* **1982**, *104*, 6895–6899. (b) La, Y. L.; Chakraborty, A. K. *J. Phys. Chem.* **1991**, *95*, 10781–10787. (c) La, Y. L.; Chakraborty, A. K. *J. Phys. Chem.* **1993**, *97*, 11291–11299.

(14) (a) Bjorling, M.; Karlstrom, G.; Linse, P. *J. Phys. Chem.* **1991**, *95*, 6706–6709. (b) Fletcher, N. C.; Ward, M. D.; Encinas, S.; Armaroli, N.; Flamigni, L.; Barigelletti, F. *Chem. Commun.* **1999**, 2089–2090. (c) Zeena, S.; Thomas, K. G. *J. Am. Chem. Soc.* **2001**, *123*, 7859–7865.

(15) (a) Andersson, M.; Karlstrom, G. *J. Phys. Chem.* **1985**, *89*, 4957–4962. (b) Cox, G. S.; Turro, N. J.; Yang, N. C.; Chen, M. J. *J. Am. Chem. Soc.* **1984**, *106*, 422–424. (c) Jiang, H.; Xu, H. *J. Chem. Soc., Perkin Trans.* **2001**, *2*, 1274–1279.

(16) Lehn, J.-M. *Supramolecular Chemistry, Concepts and Perspectives*; Wiley-VCH: Weinheim, Germany, 1995.

(17) (a) Boiocchi, M.; Del Boca, L.; Esteban- Gomez, D.; Fabbrizzi, L.; Licchelli, M.; Monzani, E. *J. Am. Chem. Soc.* **2004**, *126*, 16507–16514. (b) Boiocchi, M.; Del Boca, L.; Esteban-Gomez, D.; Fabbrizzi, L.; Licchelli, M.; Monzani, E. *Chem.—Eur. J.* **2005**, *11*, 3097–3104. (c) Esteban-Gomez, D.; Fabbrizzi, L.; Licchelli, M.; Monzani, E. *Org. Biomol. Chem.* **2005**, *3*, 1495–1500. (d) Amendola, V.; Esteban-Gomez, D.; Fabbrizzi, L.; Licchelli, M. *Acc. Chem. Res.* **2006**, *39*, 343–353. (e) Ros-Lis, J. V.; Martinez-Manez, R.; Sancenon, F.; Soto, J.; Rurack, K.; Weibhoff, H. *Eur. J. Org. Chem.* **2007**, 2449–2458. (f) Han, F.; Bao, Y.; Yang, Z.; Fyles, T. M.; Zhao, J.;

Peng, X.; Fan, J.; Wu, Y.; Sun, S. *Chem.—Eur. J.* **2007**, *13*, 2880–2892. (g) Perez-Casas, C.; Yatsimirsky, A. K. *J. Org. Chem.* **2008**, *73*, 2275–2284.

(18) Kim, S. K.; Sessler, J. L.; Gross, D. E.; Lee, C.-H.; Kim, J. S.; Lynch, V. M.; Delmau, L. H.; Hay, B. P. *J. Am. Chem. Soc.* **2010**, *132*, 5827–5836.

(19) Kumaran, R.; Ramamurthy, P. *J. Phys. Chem. B* **2006**, *110*, 23783–23789.

(20) (a) Job, P. *Ann. Chem.* **1928**, *9*, 113–203. (b) Gil, V. M. S.; Oliveira, N. C. *J. Chem. Educ.* **1990**, *67*, 473–478. (c) Loukas, Y. L. *Analyst* **1997**, *122*, 377–381.

(21) Addition of Ca^{2+} (in CD_3CN) to bichromophore **1a** (in $CDCl_3$) leads to the turbidity, due to the solubility problem, which results in the broadening of the signals.

(22) (a) Thiagarajan, V.; Ramamurthy, P.; Thirumalai, D.; Ramakrishnan, V. T. *Org. Lett.* **2005**, *7*, 657–660. (b) Thiagarajan, V.; Ramamurthy, P. *J. Lumin.* **2007**, *126*, 886–892.

(23) (a) Beer, P. D.; Hopkins, P. K.; McKinney, J. D. *Chem. Commun.* **1999**, 1253–1254. (b) Arduini, A.; Giorgi, G.; Pochini, A.; Secchi, A.; Ugozzoli, F. *J. Org. Chem.* **2001**, *66*, 8302–8308.

(24) (a) Kubik, S.; Goddard, R. *J. Org. Chem.* **1999**, *64*, 9475–9486. (b) Tozawa, T.; Misawa, Y.; Tokita, S.; Kubo, Y. *Tetrahedron Lett.* **2000**, *41*, 5219–5223. (c) Hunter, C. A.; Anderson, H. N. *Angew. Chem., Int. Ed.* **2009**, *48*, 7488–7499. (d) Willans, C. E.; Anderson, K. M.; Potts, L. C.; Steed, J. W. *Org. Biomol. Chem.* **2009**, *7*, 2756–2760.

(25) (a) Shukla, R.; Kida, T.; Smith, B. D. *Org. Lett.* **2000**, *2*, 3099–3102. (b) Gargiulli, C.; Gattuso, G.; Liotta, C.; Notti, A.; Parisi, M. F.; Pisagatti, I.; Pappalardo, S. *J. Org. Chem.* **2009**, *74*, 4350–4353.

(26) Ashokkumar, P.; Thiagarajan, V.; Vasanthi, S.; Ramamurthy, P. *J. Photochem. Photobiol. A: Chem.* **2009**, *208*, 117–124.

(27) (a) Swarc, M., Eds. In *Ions and Ion Pairs in Organic Reactions*; Wiley: New York, 1972. (b) Kaufman, M. J.; Streitwieser, A. *J. Am. Chem. Soc.* **1987**, *109*, 6092–6097.

JP107717Z